

# Structural determination of a 1/1 rational approximant to the icosahedral phase in Ti-Cr-Si alloys

J. L. Libbert and K. F. Kelton

*Department of Physics, Washington University, St. Louis, Missouri 63130*

A. I. Goldman

*Ames Laboratory and Department of Physics and Astronomy, Iowa State University, Ames, Iowa 50011*

W. B. Yelon

*University of Missouri, Research Reactor, Columbia, Missouri 65211*

(Received 13 September 1993)

We report the discovery and structural refinement of a large unit cell bcc crystalline phase in a Ti-Cr-Si alloy that is a 1/1 rational approximant to the icosahedral phase in that system. The crystal structure was determined from a Rietveld analysis of x-ray and neutron powder diffraction data. Our results demonstrate that this phase is closely related to the  $\alpha$ (Al-Mn-Si) phase, which in turn, is closely related to the structure of the icosahedral phase in the Al-transition-metal alloys. The neutron data indicate that the structure contains a significant amount of oxygen located in the Mackay clusters. Partial ordering of this oxygen may provide an explanation for the localized diffuse scattering often observed in the  $i$  phase and related crystalline phases in Ti-transition-metal alloys.

## I. INTRODUCTION

The reasons for frequent icosahedral-phase ( $i$ -phase) formation in Ti-TM-Si alloys (TM = V, Cr, Mn, Fe, Co, Ni) are not well understood. Although the  $\text{Ti}_2\text{Ni}$  structure, a fcc phase with 96 atoms in the unit cell and some atomic configurations with local icosahedral order, was originally proposed as a crystal approximant to the  $i$  phase in Ti-Fe and Ti-Ni alloys,<sup>1,2</sup> that structure does not appear in the equilibrium phase diagram of the Ti-early 3d transition-metal alloys. Further, the icosahedra in  $\text{Ti}_2\text{Ni}$  are severely distorted, reducing its usefulness as a crystal approximant. Several studies have shown that Si is essential for  $i$ -phase formation in these alloys, suggesting that one should look at the ternary phase diagrams to find a better crystal approximant.

Dong *et al.*<sup>3</sup> first reported a new, large unit cell bcc phase ( $a \approx 1.31$  nm) in rapidly quenched samples of Ti-Fe. Levine *et al.*<sup>4,5</sup> reported a similar phase as one of the annealing induced transformation products from  $i$ (TiMnSi), naming it the  $\alpha$  phase because of its apparent similarity to  $\alpha$ (AlMnSi). Selected area diffraction (SAD) studies using transmission electron microscopy (TEM) of  $\alpha$ (TiMnSi) revealed strong modulations in the intensities of the diffraction spots, giving patterns that resembled those from the  $i$  phase. Recently, the  $\alpha$  phase was reported in rapidly quenched Ti-V-Si samples,<sup>6</sup> growing with a definite orientational relation to the  $i$  phase in that system with  $\langle 100 \rangle_{\text{bcc}} \parallel \text{twofold}_i$  phase and  $\langle 111 \rangle_{\text{bcc}} \parallel \text{threefold}_i$  phase. In addition to the similarities in their diffraction patterns, suggesting similar structures, the lattice constant of the  $\alpha$  phase is related to the quasilattice constant of the  $i$  phase as predicted for a 1/1 rational approximant,<sup>7</sup>

$$a_{1/1} = a_q \left( 4 + \frac{8}{\sqrt{5}} \right)^{\frac{1}{2}},$$

where  $a_q$  is the quasilattice constant of the  $i$  phase. For  $i$ (TiCrSi),  $a_q = 4.77$  Å which yields a value of 13.13 Å for  $a_{1/1}$ , in good agreement with the value of 13.14 Å found for  $\alpha$ (TiCrSi).

Detailed structural studies of the  $\alpha$  phase in the titanium alloys discussed above are difficult since the bcc phase occurs as small grains in a multiphase mixture in the as-quenched or transformed alloys. In this paper, we report the discovery of  $\alpha$ (TiCrSi) ( $a = 1.314$  nm) in a slowly cooled alloy. We have also observed the  $\alpha$  phase in slowly cooled ingots of Ti-Mn-Si and Ti-Cr-Cu-Si. Because of its common appearance in Ti-based  $i$ -phase-forming alloys and its similarities to  $\alpha$ (AlMnSi), this phase, which appears to be stable in some systems, is likely the crystal approximant best suited for studies of  $i$ -phase formation and structure in the Ti-TM-Si alloys (TM = V, Cr, Mn, Fe). As has been demonstrated for the case of crystal approximants in the Al-TM  $i$  phases, a knowledge of the structure of this phase will provide insight into the structure of titanium-based icosahedral phases. Further, since conventional tight-binding methodologies can be used for the transition-metal alloys, these Ti-TM-Si alloys might provide better systems for theoretical studies of stability and of electronic and transport properties.

We report the results of a Rietveld analysis based on x-ray and neutron powder data obtained from single-phase samples of  $\alpha$ (TiCrSi), giving the atomic positions and site occupancies in this new phase. We show that it is a true bcc version of the  $\alpha$ (AlMnSi) phase. We also demonstrate that oxygen sits randomly in octahedral sites be-

tween the first and second shells of the Mackay icosahedra clusters in this phase and between the two clusters along the  $\langle 111 \rangle$  direction of the bcc structure which may explain the diffuse scattering generally observed in the titanium-based icosahedral phases. This is the first determination of the structure of any crystalline approximant to a titanium-based quasicrystal.

## II. EXPERIMENT

Ingots of nominal composition  $\text{Ti}_{60}\text{Cr}_{25}\text{Si}_{15}$  were prepared by rf-induction melting Ti(99.5% pure), Cr(99.99% pure), and Si(99.999% pure) in zirconia coated fused silica crucibles. The as-processed Ti had at most 0.15 at.% oxygen present. The sample was melted and cooled in a vacuum chamber that was first pumped to  $10^{-5}$  torr and then backfilled with 1 atm of argon. The as-cast material was a mixture of several crystalline phases, though most of the ingot consisted of a large unit cell bcc phase. Annealing the as cast ingots at  $1175^\circ\text{C}$  for 1 week in an argon atmosphere resulted in a single-phase sample consisting entirely of the large unit cell bcc phase. X-ray powder studies were carried out on two instruments: a Siemens type F and a Phillips diffractometer, both using the Bragg-Brentano geometry employing  $\text{Cu-K}\alpha$  radiation. Each instrument was equipped with a post-sample monochromator. The sample microstructure, diffraction, and local composition were studied using a JEOL 2000-FX transmission electron microscope equipped with a Tracor-Northern energy dispersive spectrometer (EDS). Neutron powder data was collected on the high resolution powder diffractometer at the University of Missouri Research Reactor (MURR). The sample was contained in a 3.2 mm diameter thin walled vanadium cell. This instrument uses a bent Si crystal monochromator to produce neutrons with  $\lambda = 1.7651 \text{ \AA}$ . The data were collected at room temperature using a linear position sensitive detector spanning  $20^\circ$  and were rebinned into  $0.05^\circ$  steps. The detector therefore spans the  $100^\circ$  ( $2\theta$ ) range in five intervals. Data were acquired over a period of 2 days. Density measurements were obtained by immersion weighing in toluene using a Cahn microbalance. The structure was refined using the GSAS (general structure analysis system) which performs a Rietveld analysis on x-ray or neutron powder data.<sup>8</sup>

## III. TEM AND DIFFRACTION RESULTS

The slowly cooled ingots of  $\text{Ti}_{75-x}\text{Cr}_{25}\text{Si}_x$ , ( $\text{Si} > 10 \text{ at.}\%$ ) were strongly faceted. An examination of these ingots by x-ray diffraction indicated that although they contained a mixture of several crystalline phases, a major fraction of the sample consisted of a 1.314 nm bcc phase. Its diffraction pattern is strikingly similar to that for  $i(\text{TiCrSi})$ . Figure 1 contrasts the x-ray diffraction spectrum from a single-phase  $i(\text{TiCrSi})$  sample with that from  $\alpha(\text{TiCrSi})$ . The (211111) peak (Elser scheme) (Ref. 9) in the  $i$ -phase sample matches closely the position and intensity of the (530) peak in the bcc phase, the  $i$ -phase

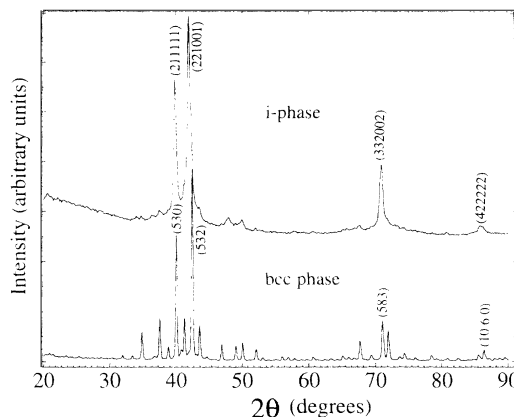


FIG. 1. X-ray diffraction data from the icosahedral phase Ti-Cr-Si obtained by rapid quenching (top) and the bcc phase from an annealed ingot (bottom). The  $i$ -phase pattern is indexed according to the scheme of Elser (Ref. 9).

(221001) peak corresponds to the (532) crystalline peak, and the (332002) peak appears at the position of the (583) bcc peak. These similarities demonstrate that the local atomic configurations of the two phases are closely related. This similarity is also confirmed by SAD studies of the  $i$  phase and the  $\alpha$  phase. Figure 2(a) shows the SAD taken along an  $i$ -phase twofold direction and Fig. 2(b) shows the SAD taken along the bcc [100] zone. The most intense spots in the bcc SAD match those observed in the  $i$ -phase diffraction pattern both in intensity and position; the (211111) peak matches the (035) bcc

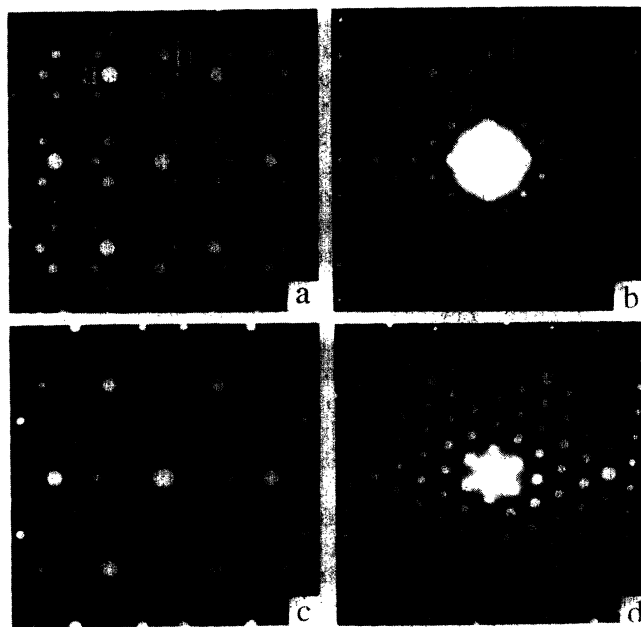


FIG. 2. Selected area diffraction patterns of the  $i$  phase and bcc phase along certain high symmetry axes: (a)  $i$ -phase twofold [100]; (b) bcc [100] axis. The (035) crystalline peak (c) corresponds to the (100000)  $i$ -phase peak (a), and the (006) bcc spot (d) matches the (110000)  $i$ -phase spot (b). (c)  $i$ -phase threefold, (d) bcc [111] axis.

peak; the (221001) peak matches the (006) bcc peak, though it is shifted slightly towards a larger  $d$  spacing, consistent with the x-ray data. Figures 2(c) and 2(d) show SAD patterns taken along the  $i$ -phase threefold zone and along the [111] zone of the cubic approximant; again the patterns are similar. These intensity modulations are the same as those noted in Ti-V-Si materials where the bcc phase was found growing coherently with the  $i$  phase.<sup>6</sup>

EDS studies place the composition of the bcc phase at  $\text{Ti}_{75-x}\text{Cr}_{25}\text{Si}_x$  with  $10 < x < 20$ ; Si appears to substitute preferentially for Ti. The Cr concentration varied by only 2 or 3%. This composition is comparable to that found for  $i(\text{TiVSi})$  and  $i(\text{TiCrSi})$ ,  $\text{Ti}_{73-x}\text{V}_{27}\text{Si}_x$  ( $13 < x < 25$ ) and  $\text{Ti}_{68-x}\text{Cr}_{32}\text{Si}_x$  ( $6 < x < 18$ ) respectively.<sup>6,10</sup>

Figures 3(a) and 3(b) show x-ray and neutron data, respectively, from a sample of Ti-Cr-Si that had been annealed at 1175 °C for 1 week in an argon atmosphere to obtain a single-phase bcc sample. All lines can be indexed to the 1.314 nm phase. The fits to the data are based on a structural model developed in the next section.

#### IV. RIETVELD ANALYSIS OF DIFFRACTION RESULTS

There are two well-known examples of 1/1 approximants in the aluminum-based icosahedral alloys. One of these, the Bergman phase,  $(\text{Al,Zn})_{49}\text{Mg}_{32}$ ,<sup>11</sup> is nearly isostructural to the  $R\text{-Al}_5\text{LiCu}_3$  phase, which has been shown to be structurally related to the stable  $i$  phase  $\text{Al}_6\text{LiCu}_3$ .<sup>12,13</sup> The  $R$  phase is bcc with a lattice constant of 1.389 nm consisting of two icosahedral clusters (Pauling triacontrahedra), one located at the cell origin and another at the cell center connected by their edges along the cube edges and by threefold faces in the  $\langle 111 \rangle$  directions.

The other 1/1 approximant is  $\alpha(\text{AlMnSi})$ .<sup>14</sup> This phase also has identical clusters with icosahedral symmetry located at the cell corners and center, though the clusters differ from those found in the Bergman phase. The clusters relevant to this phase are the Mackay icosahedra. Surrounding these clusters are "glue" atoms that fill the unit cell and form the connections between the clusters. Since some of the glue sites that are filled at the cell cor-

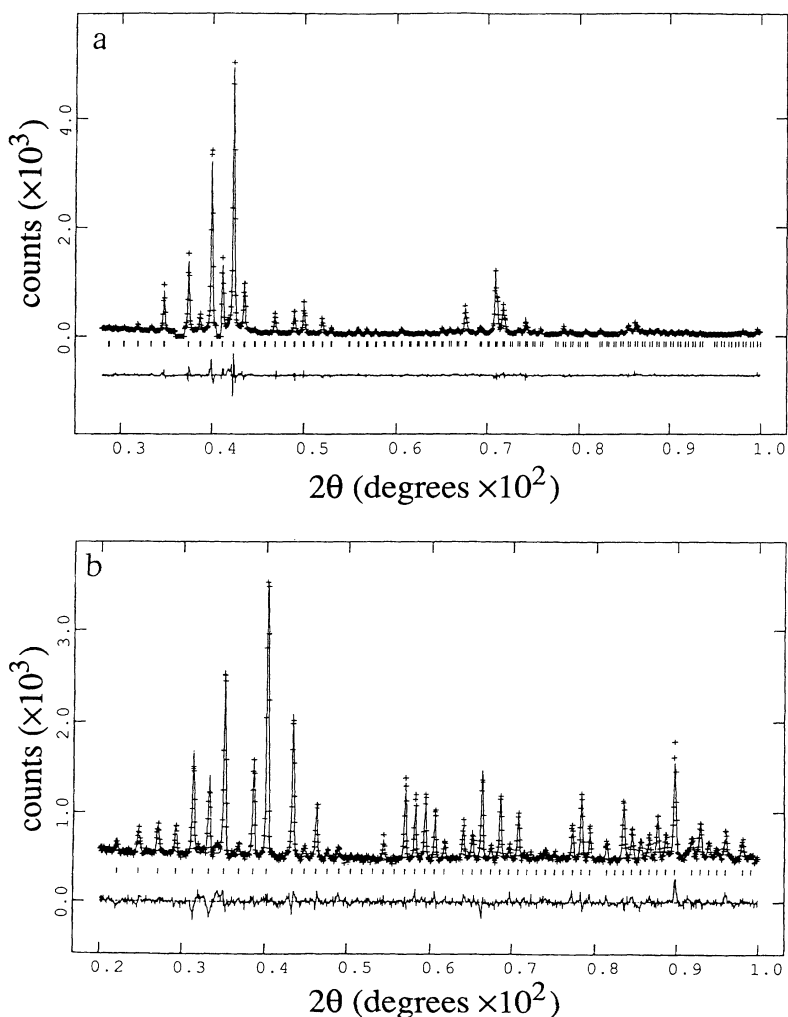


FIG. 3. The  $\alpha(\text{TiCrSi})$  diffraction data (+) and the fit (solid line) for both x rays (a) and neutrons (b) as described in the text. At the bottom of each plot is the difference curve for the fit. For the x-ray data  $\lambda = 1.54056 \text{ \AA}$  and for the neutron data  $\lambda = 1.7651 \text{ \AA}$ .

ners are not occupied at the cell centers in  $\alpha(\text{AlMnSi})$ , the space group is actually  $Pm\bar{3}$ . A bcc version of this phase ( $Im\bar{3}$ ) exists in Al-Fe-Si alloys, however.<sup>15</sup>

As a starting point for the refinement based on fits to the x-ray and neutron data (Fig. 3), a reasonable decoration was determined for each of these structures using the correct stoichiometry and taking into account the relative sizes of the atoms. The initial positions of the atoms for the  $R$  phase were taken from Ref. 12 and atom positions for the  $\alpha(\text{AlMnSi})$  phase were taken from Ref. 14. During the refinement the numbers of the various atoms were constrained to match fairly closely the composition as determined by EDS.

In crystallographic refinements the fits are characterized by the residuals  $wR_p$ ,  $R_p$ , and  $\chi^2$ , providing a standard measure of how well the calculated data match the observed data. In the general structural analysis system (GSAS) they are defined as

$$R_p = \frac{\sum |I_o - I_c|}{\sum I_o},$$

$$wR_p = \sqrt{\frac{M}{\sum wI_o^2}},$$

where

$$M = \sum w(I_o - I_c)^2.$$

The reduced  $\chi^2$  is given by

$$\chi^2 = \frac{M}{(N_{\text{obs}} - N_{\text{var}})}.$$

$I_o$  and  $I_c$  are the observed and calculated integrated intensities, respectively, and  $w$  is a weighting factor. For crystallographic refinements  $\chi^2$  usually ranges between 2 and 4. The minimum values for the residuals depends upon the statistical accuracy of the data to be fit and are determined by the GSAS program. For the x-ray data the minimum possible  $wR_p$  was 0.095. The neutron data minimum for  $wR_p$  was 0.045.

Several different decorations were tried assuming the  $R$ -phase structure but none were found that gave reasonable results. The best fit for that structure resulted in a  $\chi^2$  of 13 and  $wR_p$  of 0.20. Much better results were obtained by starting with the atomic positions for the  $\alpha(\text{AlMnSi})$  structure. For the x-ray fit  $\chi^2 = 1.92$ ,  $wR_p = 0.117$ , while for the neutron fit  $\chi^2 = 1.77$ ,  $wR_p = 0.054$ , all near the statistical limit. Fitting both data sets simultaneously resulted in an overall  $\chi^2$  of 2.1, with  $wR_p = 0.12$  for the x-ray data and  $wR_p = 0.054$  for the neutron data.

Table I shows the atomic site positions and decoration for  $\alpha(\text{TiCrSi})$  determined from the fits to the diffraction data. The atomic positions and decorations shown were determined by fitting to the x-ray and neutron data simultaneously. Though these positions are in reasonable agreement with the atomic positions reported in an earlier study<sup>16</sup> involving only x-ray data, there are some differences. The x-ray atomic form factors for Ti and Cr are very similar, giving ambiguous results when the

TABLE I. Atomic positions in fractional coordinates and fractional occupancies for the  $\alpha(\text{TiCrSi})$  phase, as determined by the Rietveld analysis described in the text. The results shown were obtained by fitting the x-ray and neutron data simultaneously. A typical standard deviation for the positions is 0.0005.

Atom positions and occupancies in $\alpha(\text{TiCrSi})$					
<i>cI146</i>	Space group $Im\bar{3}$			$a = 1.3139$ nm	
Site	<i>x</i>	<i>y</i>	<i>z</i>	Occupancy	
1 2( <i>a</i> )	0	0	0	0.27 Cr, 0.73 Si	
2 24( <i>g</i> )	0	0.1761	0.1082	1 Ti	
3 24( <i>g</i> )	0	0.3416	0.2168	0.45 Cr, 0.55 Si	
4 48( <i>h</i> )	0.1135	0.1831	0.3047	1 Ti	
5 12( <i>d</i> )	0.3810	0	0	1 Ti	
$\gamma$ 24( <i>g</i> )	0	0.3399	0.4026	0.66 Cr, 0.16 Si, 0.18 Ti	
$\delta$ 12( <i>e</i> )	0	0.5	0.3258	0.58 Cr, 0.42 Si	
7 8( <i>c</i> )	0.250	0.250	0.250	0.90 O	
8 24( <i>g</i> )	0.2433	0	0.0952	0.67 O	

atoms are exchanged on various sites. The neutron scattering lengths for these two atoms, however, are quite dissimilar making it possible to decide easily whether the site is occupied by Ti or Cr. In addition, neutrons make it possible to detect light atoms that might be present in the structure, but which are invisible to x rays due to their small scattering factors. Both x-ray and neutron data are therefore essential to determining the best decoration for this phase. Figure 3 shows the results of the fits for the x-ray [Fig. 3(a)] and neutron [Fig. 3(b)] data. The data are indicated by (+) and the calculated patterns are shown as solid lines. The difference curve for the fits is shown below each plot. In both cases the calculated patterns and the data agree well.

## V. DISCUSSION

Table I shows the crystallographic site locations and the atomic decoration of these sites. As in  $\alpha(\text{AlMnSi})$ , the main structural unit in  $\alpha(\text{TiCrSi})$  is the Mackay icosahedron (MI). In  $\alpha(\text{TiCrSi})$  this cluster consists of a central Cr or Si atom surrounded by 12 Ti atoms forming a small icosahedron. A second, double-sized, icosahedron is formed by placing 12 Cr/Si atoms directly out from the vertices of the small Ti icosahedron. Finally 30 Ti atoms are placed just outside the edges of the double sized Cr/Si icosahedron, completing the 55-atom cluster (Fig. 4). Two MI are in each unit cell, one at the cube corner and another at the center stacked along the  $\langle 111 \rangle$  directions separated by an octahedron, so that they maintain the same orientation throughout the structure. These clusters are then surrounded by a layer of "glue" atoms that fill the unit cell and form the linkages between the clusters.

This structure differs from that of  $\alpha(\text{AlMnSi})$  in two important respects. First, it should be noted that in  $\alpha(\text{AlMnSi})$  the center of the MI are empty while they are filled in this phase. This agrees with studies that show a high vacancy formation energy in Ti alloys.<sup>17</sup> Secondly, in the AlMnSi phase, Al and Si are believed to substitute

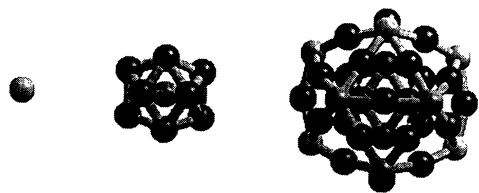


FIG. 4. The Mackay cluster as it appears in the  $\alpha(\text{TiCrSi})$  phase. A central Cr/Si atom is surrounded by 12 Ti atoms at the vertices of a small icosahedron. Cr/Si atoms sit straight out from the vertices of the small icosahedron forming a double-sized icosahedron. Ti atoms are situated slightly out from the edges of this double-sized icosahedron completing the 55-atom Mackay cluster.

for one another on the small icosahedra and at the edge sites. On the basis of the neutron data for  $\alpha(\text{TiCrSi})$ , the Si substitutes for the Cr atoms, leaving only Ti on the small icosahedra and edge sites. This is reasonable since Si is closer in size to Cr than it is to Ti. Composition studies across the  $i$ -phase-forming range, however, suggest that the Si substitutes preferentially for Ti. It may be that the Si substitutes for Cr until all small sites are filled after which it substitutes for the Ti. It should be noted that at least 10 at. % silicon is needed to form  $\alpha(\text{TiCrSi})$ .

On the basis of the neutron data it was determined that there is a significant amount of oxygen present in these Mackay icosahedra. Oxygen atoms are located at 12 of the 20 faces of the small Ti icosahedra in the octahedral sites between the inner and outer shells of the MI with an occupancy of 0.68. The eight faces along the  $\langle 111 \rangle$  directions are not filled. Instead, oxygen atoms are located at  $\{\frac{1}{4}, \frac{1}{4}, \frac{1}{4}\}$  which are the eight equivalent octahedral sites between the two MI along the  $\langle 111 \rangle$  direction. These oxygen atoms were necessary to obtain reasonable fits to the neutron diffraction data; without it the best fit to the neutron data yielded a  $\chi^2$  of 9.0 and  $wR_p$  of 0.13. In addition, several of the sites in the neutron fits deviated significantly from their positions determined by the x-ray fits. For example the small Ti icosahedron determined from fitting the x-ray data was only slightly distorted from true icosahedral symmetry. This icosahedral symmetry was strongly distorted in the fits to the neutron data if the oxygen were not included, but was in good agreement with the x-ray fits when oxygen atoms were located above the faces of the small icosahedron. The  $\gamma$  sites, one of the glue atom sites, were strongly influenced by the presence of oxygen. From both the x-ray and neutron fits the 12 atoms in these sites formed polyhedra of the same shape. The positions given by the fits to the neutron data without including oxygen, however, were moved closer to the origin, resulting in unphysically short bonds. Again when the oxygen atoms were placed as before, the positions of the  $\gamma$  sites relaxed to those determined from the x-ray data.

Density measurements also suggest that oxygen is present. The calculated density of  $\alpha(\text{TiCrSi})$  using only Ti, Cr, and Si in the correct stoichiometry is  $4.90 \text{ g cm}^{-3}$ . The measured density is  $5.11 \pm 0.05 \text{ g cm}^{-3}$ . With oxy-

gen included in the amounts indicated by the neutron fits, the calculated density rises to  $5.16 \text{ g cm}^{-3}$ , in much better agreement with the measured value. The oxygen which appears in this phase most likely enters the sample during the melting and subsequent cooling as contamination from the fused silica crucibles. It is not known at this time whether the oxygen plays an important role in the stabilization and structural perfection of the  $\alpha(\text{TiCrSi})$  and related icosahedral phases.

While the occupancy of the oxygen sites on the Mackay icosahedra in the crystalline  $\alpha(\text{TiCrSi})$  phase studied here is high, a larger number of vacancies and less order might exist in the icosahedra presumably present in the rapidly quenched Ti-based icosahedral phases. It is well known that oxygen disorder can give rise to localized diffuse scattering in crystalline alloys. Oxygen, then might provide the key to understanding the localized diffuse scattering often observed in those quasicrystals.<sup>18,19</sup> Since the oxygen sites have an icosahedral symmetry, the location of the diffuse scattering due to a disorder in the occupation of these sites would follow the icosahedral symmetry of the quasicrystal, as is experimentally observed.

Since  $\alpha(\text{TiCrSi})$  is a true bcc phase we can describe the structure by the arrangement of the atoms about the cell origin. As mentioned earlier a MI is centered at the origin and the body center. Surrounding the MI are the so-called "glue" atoms designated as  $\delta$  and  $\gamma$  sites in Table I. It is worth noting that the six  $\delta$  sites that are associated with each cluster form one-half of an icosahedron that has the same orientation as the double-sized Cr icosahedron of the MI. These atoms are shared by the clusters adjoining along the cube edges. Thus the  $\delta$  sites, considered by themselves, form edge connected icosahedra along the  $\langle 100 \rangle$  directions. Along the  $\langle 111 \rangle$  direction the icosahedra formed by the  $\delta$  sites at the center and origin interpenetrate on the threefold face. The 12  $\gamma$  sites on each cluster could be described as a severely distorted icosahedron since there is a  $\gamma$  site associated with each of the 12 vertices of the  $\delta$  site icosahedron, but the  $\gamma$  sites actually sit in the faces of the  $\delta$  site icosahedron, in a pocket formed by an atom at the vertex of the double-

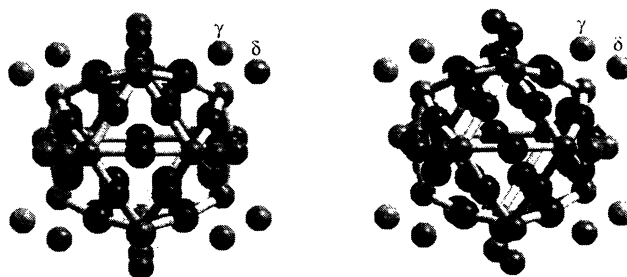


FIG. 5. Stereo pair showing the positions of the  $\gamma$  and  $\delta$  sites with respect to the second Mackay shell. The  $\delta$  atoms lie nearly on line with the vertices of the second Mackay icosahedron, thus they form a third large icosahedron when considered by themselves. The  $\gamma$  sites are situated in the face formed by an atom at the vertex of the double-sized icosahedron and two adjacent edge sites. These  $\gamma$  sites are shared with clusters in the body diagonal directions.

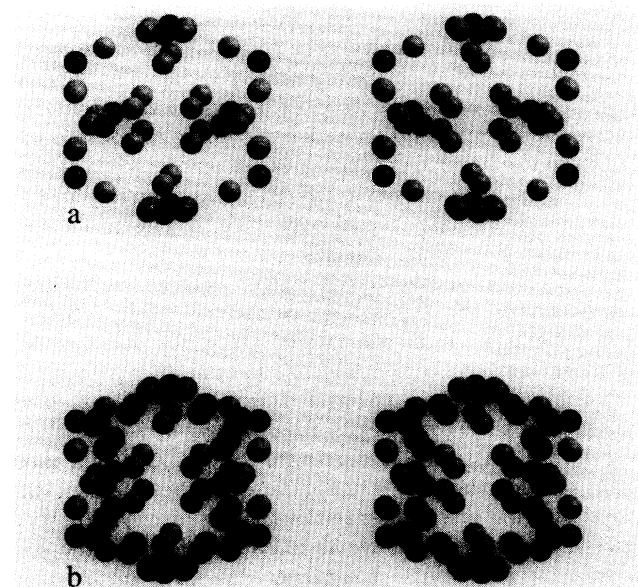


FIG. 6. (a) Stereo pair of the third shell which surrounds each Mackay cluster in  $\alpha(\text{TiCrSi})$  as viewed along the (100) direction. The atoms in the  $\delta$  sites are the dark atoms. They sit at the vertices of a large icosahedron. Three  $\gamma$  atoms sit on each of the non- $\langle 111 \rangle$  faces of this large icosahedron. (b) Atoms from the edges of the second Mackay shell of the eight neighboring body diagonal clusters (Ti atoms) fill the faces in the  $\langle 111 \rangle$  directions.

sized Mackay shell and two adjoining edge sites (Fig. 5). There are three such locations on each face of the  $\delta$  icosahedron. One of these is filled by the  $\gamma$  atom associated with the central cluster. The other two sites are filled by  $\gamma$  atoms from neighboring clusters in the body diagonal directions [Fig. 6(a)].

Only 12 of the 20 faces of the  $\delta$  icosahedron have  $\gamma$  sites on them. The empty faces are the faces along the  $\langle 111 \rangle$  directions. Along these directions the interpenetration of the  $\delta$  shells is such that three atoms at the edges of the second Mackay shell of the neighboring clusters along the body diagonals fall in these faces. The overall result is a completed third shell that has pseudoicosahedral symmetry [Fig. 6(b)].

This shell also exists in the  $\alpha(\text{AlMnSi})$  phase as described by Fowler *et al.*<sup>20</sup> It is less symmetric in  $\alpha(\text{TiCrSi})$  than in  $\alpha(\text{AlMnSi})$  because the edge sites of the second Mackay shell are Ti atoms while the  $\gamma$  atoms

are mainly Cr/Si. Thus while each vertex of the  $\delta$  icosahedron is surrounded by five atoms, two of them are Ti and three are Cr/Si, destroying the fivefold rotation symmetry of the cluster. The atoms in the edge sites also form a smaller triangle than the triangle formed by the  $\gamma$  sites, further distorting this shell. This distortion is clear in Fig. 6. Thus the main skeleton of the structure can be described as three icosahedral shells, the first two forming a two-shell Mackay icosahedron while the third shell consisting of the glue atoms and some second shell edge sites is of distorted icosahedral symmetry, interpenetrating along threefold faces in the  $\langle 111 \rangle$  directions and joined by edges along the cube edge directions.

## VI. CONCLUSION

We have discovered a large unit cell bcc phase in Ti-Cr-Si alloys that is a 1/1 rational approximant to the  $i$  phase. The structure of the phase was determined by a Rietveld analysis using x-ray and neutron diffraction data. It is quite similar to the  $\alpha(\text{AlMnSi})$  phase, except the centers of the Mackay and the normally vacant " $\delta$ " sites are filled, making  $\alpha(\text{TiCrSi})$  a true bcc structure. The neutron scattering experiments also indicate that a significant amount of oxygen is present in the Mackay cluster, which may help explain the intense arcs of diffuse scattering commonly found in Ti-TM-Si  $i$  phases and their approximants. This is the first determination of the structure of a crystalline approximant to the  $i$  phase in Ti-TM-Si alloys and will lead to a better understanding of  $i$ -phase formation in these systems.

## ACKNOWLEDGMENTS

The authors thank X. Zhang, T. L. Daulton, P. C. Gibbons, A. E. Carlsson, and L. E. Levine for enlightening discussions and assistance. We also thank M. Kramer for assistance with the Rietveld analysis, and thank J. Shields for assistance in acquisition of some of the x-ray data. The images were created using MacMolecule ©University of Arizona. This work was partially supported by NSF Grant No. DMR 92-03052, Ames Laboratory is operated for the U.S. Department of Energy by Iowa State University under Contract No. W-7405-ENG-85.

<sup>1</sup> Z. Zhang, H. Q. Ye, and K. H. Kuo, *Philos. Mag. A* **52**, L49 (1985).

<sup>2</sup> C. Dong, Z. K. Hei, L. B. Wang, Q. H. Song, Y. K. Wu, and K. H. Kuo, *Scr. Metall.* **20**, 1155 (1986).

<sup>3</sup> C. Dong, K. Chattopadhyay, and K. H. Kuo, *Scr. Metall.* **21**, 1307 (1987).

<sup>4</sup> L. Levine, J. C. Holzer, P. C. Gibbons, and K. F. Kelton, *Philos. Mag. B* **65**, 435 (1992).

<sup>5</sup> J. C. Holzer, K. F. Kelton, L. E. Levine, and P. C. Gibbons, *Scr. Metall.* **23**, 691 (1989).

<sup>6</sup> X. Zhang and K. F. Kelton, *Philos. Mag. Lett.* **63**, 39 (1991).

<sup>7</sup> V. Elser and C. L. Henley, *Phys. Rev. Lett.* **55**, 2883 (1985).

<sup>8</sup> H. M. Rietveld, *J. Appl. Cryst.* **2**, 65 (1969).

<sup>9</sup> V. Elser, *Phys. Rev. B* **32**, 4892 (1985).

<sup>10</sup> X. Zhang and K. F. Kelton, *Philos. Mag. Lett.* **62**, 265 (1990).

<sup>11</sup> G. Bergman, J. T. Waugh, and L. Pauling, *Acta Crystallogr.* **10**, 157 (1957).

<sup>12</sup> C. H. Guryan, P. W. Stephens, A. I. Goldman, and F. W.

- Gayle, Phys. Rev. B **37**, 8495 (1988).
- <sup>13</sup> M. Audier, J. Pannetier, M. Lebranc, C. Janot, J. Lang, and B. Dubost, Physica B **153**, 136 (1988).
- <sup>14</sup> M. Cooper and K. Robinson, Acta Crystallogr. **20**, 614 (1966).
- <sup>15</sup> M. Cooper, Acta Crystallogr. **23**, 1106 (1967).
- <sup>16</sup> J. L. Libbert, K. F. Kelton, and A. I. Goldman, J. Non-Cryst. Solids **153&154**, 53 (1993).
- <sup>17</sup> A. E. Carlsson (private communication).
- <sup>18</sup> P. C. Gibbons, K. F. Kelton, L. E. Levine, and R. B. Phillips, Philos. Mag. B **59**, 593 (1989).
- <sup>19</sup> K. F. Kelton and P. C. Gibbons, Philos. Mag. B **66**, 639 (1992).
- <sup>20</sup> H. A. Fowler, B. Mozer, and J. Sims, Phys. Rev. B **37**, 3906 (1988).

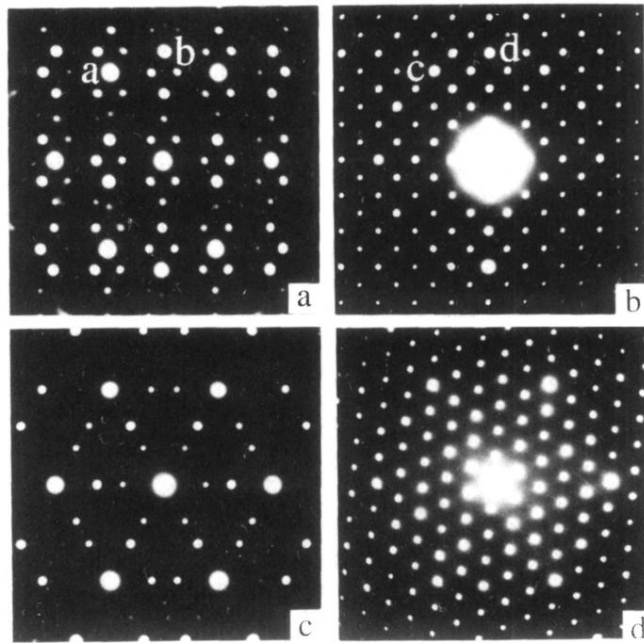


FIG. 2. Selected area diffraction patterns of the *i* phase and bcc phase along certain high symmetry axes: (a) *i*-phase twofold [100]; (b) bcc [100] axis. The (0 $\bar{3}$ 5) crystalline peak (c) corresponds to the (100000) *i*-phase peak (a), and the (006) bcc spot (d) matches the (110000) *i*-phase spot (b). (c) *i*-phase threefold, (d) bcc [111] axis.



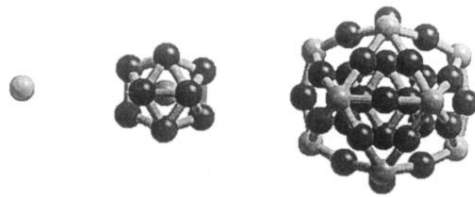


FIG. 4. The Mackay cluster as it appears in the  $\alpha(\text{TiCrSi})$  phase. A central Cr/Si atom is surrounded by 12 Ti atoms at the vertices of a small icosahedron. Cr/Si atoms sit straight out from the vertices of the small icosahedron forming a double-sized icosahedron. Ti atoms are situated slightly out from the edges of this double-sized icosahedron completing the 55-atom Mackay cluster.

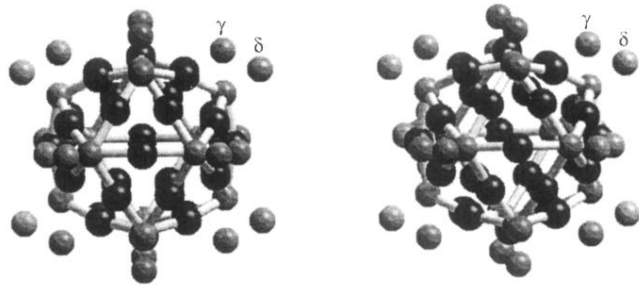


FIG. 5. Stereo pair showing the positions of the  $\gamma$  and  $\delta$  sites with respect to the second Mackay shell. The  $\delta$  atoms lie nearly on line with the vertices of the second Mackay icosahedron, thus they form a third large icosahedron when considered by themselves. The  $\gamma$  sites are situated in the face formed by an atom at the vertex of the double-sized icosahedron and two adjacent edge sites. These  $\gamma$  sites are shared with clusters in the body diagonal directions.

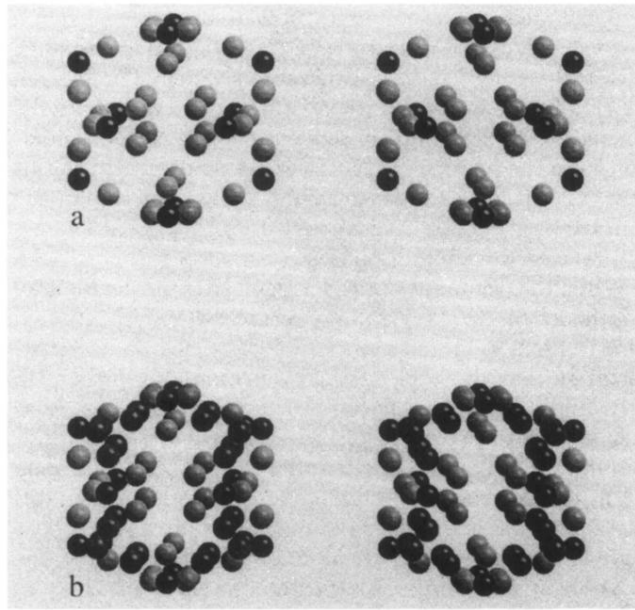


FIG. 6. (a) Stereo pair of the third shell which surrounds each Mackay cluster in  $\alpha(\text{TiCrSi})$  as viewed along the (100) direction. The atoms in the  $\delta$  sites are the dark atoms. They sit at the vertices of a large icosahedron. Three  $\gamma$  atoms sit on each of the non- $\langle 111 \rangle$  faces of this large icosahedron. (b) Atoms from the edges of the second Mackay shell of the eight neighboring body diagonal clusters (Ti atoms) fill the faces in the  $\langle 111 \rangle$  directions.